ISSN 1061-9348, Journal of Analytical Chemistry, 2006, Vol. 61, No. 9, pp. 902–911. © Pleiades Publishing, Inc., 2006.
Original Russian Text © S.V. Kharitonov, 2006, published in Zhurnal Analiticheskoi Khimii, 2006, Vol. 61, No. 9, pp. 975–984.

ARTICLES

Membrane Drotaverine-Selective Electrodes Based on Tetraphenylborate Derivatives: Electrochemical, Adsorption, and Transport Properties and Analytical Application

S. V. Kharitonov

St. Petersburg State Technological Institute (Technical University), Moskovskii pr. 26, St. Petersburg, 190013 Russia

Received May 4, 2005; in final form, July 20, 2005

Abstract—The potentiometric response of ion-selective electrodes (ISEs) based on different lipophilic derivatives of tetraphenylborate to drotaverine hydrochloride was studied. The composition of a polymeric membrane was optimized to obtain the best electroanalytical properties of ISEs. The transport properties of selective membranes, the permeability and the flow of ions through the interface, were studied. Linear correlations between the solubility of ionophoric membrane components, membrane transport, and electroanalytical properties were revealed. The kinetic studies of ion-exchange adsorption showed that two limiting stages of transfer, namely, diffusion through the boundary layer and diffusion through the membrane phase, occurred. Procedures for the potentiometric determination of drotaverine hydrochloride in pharmaceutical forms were proposed.

DOI: 10.1134/S1061934806090115

Drotaverine or 1-(3,4-diethoxybenzylidene)-6,7-diethoxy-1,2,3,4-tetraisoquinoline

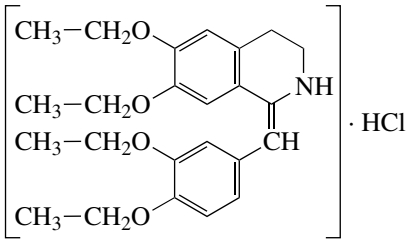

is widely used in medicine as an effective spasmolytic agent from the group of isoquinoline spasmolytics [1].

The determination of drotaverine hydrochloride by high-performance liquid chromatography (HPLC) was described in [2, 3]. The procedure is rather accurate and rapid but requires expensive and, in some cases, difficult to obtain equipment.

Potentiometry is a simple and available method for determining organic compounds. It allows the concentration of pharmaceuticals to be determined in ready-made drugs, industrial chemicopharmaceutical raw products and semiproducts, blood, serum, and some other materials using ion-selective electrodes.

The state-of-the-art applied potentiometry requires that both theoretical investigations dedicated to elucidating the selectivity nature of electrode membranes be extended and new methods of their synthesis and modification be sought to obtain a more perfectly structurally organized membrane and to widen its functional properties. For this purpose, it is necessary to find correlations between electrochemical, transport, and adsorption properties of membranes and their effect on ISE properties.

The goal of this work was to develop ISEs reversible to the 1-(3,4-diethoxybenzylidene)-6,7-diethoxy-1,2,3,4-tetraisoquinoline cation based on different lipophilic derivatives of tetraphenylborate. We analyzed the effect of the ionophore solubility on the linearity range of the ISE response, calculated permeability coefficients and the flow of ions, and studied dynamic and adsorption properties of selective membranes. Procedures for determining the pharmaceutical of interest by potentiometry and potentiometric precipitation titration were proposed.

EXPERIMENTAL

The following reagents were used: a substance of drotaverine hydrochloride ($[C_{24}H_{32}O_4N]^+Cl^-$) (DH) of pharmacopeial grade from Nanjing Pharmaceutical Factory; tetraphenylborate derivatives synthesized by the procedure given below; dibutyl phthalate (DBP); cyclohexanone; S-70 polyvinyl chloride (PVC). All reagents were of analytical or cp grade. DBP was purified by double distillation in vacuum.

Sodium tetraphenylborate and its derivatives, tetrakis(*p*-chlorophenyl)borate $Na[B(C_6H_4Cl)_4]$, tetrakis(*p*-methylphenyl)borate $Na[B(C_6H_4CH_3)_4]$, and tetrakis[3,5-bis(trifluoromethyl)phenyl]borate $Na[B\{C_6H_3(CF_3)_2\}_4]$ were synthesized by the following reaction:

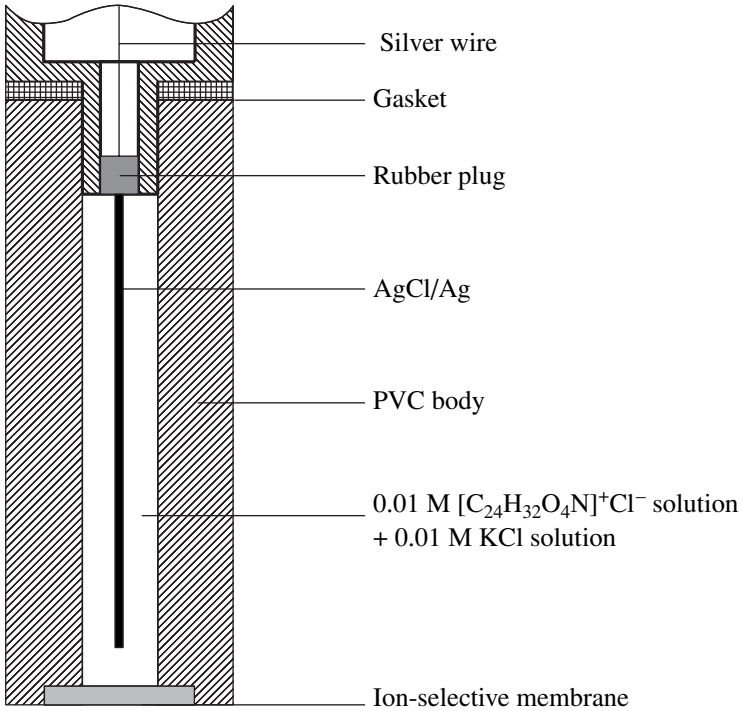

Fig. 1. ISE design.

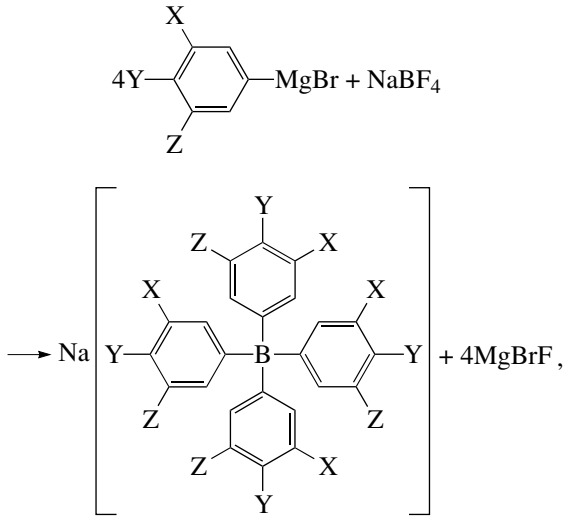

where X, Y, and Z are H, Cl, CH_3, or CF_3.

A finely divided $NaBF_4$ powder was added to an ether solution of the Grignard reagent. The reaction was performed in a flask supplied with a petal-shaped stirrer and a reflux condenser. The reaction mixture was heated on a water bath for 1.5–4 h in nitrogen atmosphere. After cooling, it was filtered through a glass filter. The residue on the filter was washed three or four times with absolute ether. The resulting product was recrystallized from ether or acetone.

A 5×10^{-2} M drotaverine hydrochloride stock solution was prepared in twice-distilled water from an accurately weighed sample. Solutions of lower concentrations (1×10^{-2}–1×10^{-7} M) were prepared by successively diluting the stock solution. Ionophores for ISE membranes were obtained by precipitating drotaverine hydrochloride from its aqueous solutions containing tetraphenylborate derivatives. The precipitates were separated by centrifuging and dried in a vacuum desiccator at room temperature.

Plasticized membranes contained 30 wt % PVC and 70 wt % DBP. The ionophore concentration in DBP was varied from $n \times 10^{-2}$ to $n \times 10^{-4}$ mol/kg DBP. Before use, ISEs were conditioned in a 1×10^{-3} M $[C_{24}H_{32}O_4N]^+Cl^-$ solution for 1 h. The design of the ISE is presented in Fig. 1.

The electrode characteristics of ISEs were measured using the following electrochemical cell:

Ag| AgCl | 1×10^{-2} M DH solution + 1×10^{-2} M KCl solution | Ion-selective membrane | Test solution || Saturated KCl solution | AgCl | Ag.

The measurements were made using a computerized instrument based on a Svet-PI-1 potentiometric transducer (OOO Spektrum, St. Petersburg). The accuracy of potentiometric measurements was verified by HPLC using an integrated Summit® HPLC Analytical System module.

The potentiometric selectivity coefficients of ISEs were determined by the mixed-solution method for inorganic cations or by the separate-solution method for organic cations.

Table 1. Solubility products of ionophores

Structural unit of ion exchanger	K_S^{IS}
$[C_{24}H_{32}O_4N]^+[B(C_6H_5)_4]^-$	$(3.7 \pm 0.3) \times 10^{-12}$
$[C_{24}H_{32}O_4N]^+[B(C_6H_4CH_3)_4]^-$	$(3.4 \pm 0.4) \times 10^{-13}$
$[C_{24}H_{32}O_4N]^+[B(C_6H_4Cl)_4]^-$	$(4.6 \pm 0.5) \times 10^{-14}$
$[C_{24}H_{32}O_4N]^+[B\{C_6H_3(CF_3)_2\}_4]^-$	$(2.4 \pm 0.5) \times 10^{-15}$

Because the 1-(3,4-diethoxybenzylidene)-6,7-diethoxy-1,2,3,4-tetraisoquinoline cation can absorb light in the UV spectral region (molar absorption coefficient ε is about 20 000 at λ_{max} = 260.0 nm), solubility products of ion exchangers (K_S^{IS}) were calculated from spectrophotometric data obtained with a Specord M-40 spectrophotometer for equilibrium concentrations of DH in the solution above the precipitate using the previously constructed calibration graphs.

The stability of the ISE potentials and electrochemical properties of membranes (electric conductivity and permittivity) were estimated from conductometric data obtained by applying sinusoidal pulses of alternate voltage 10 V in amplitude to the cell. The overall resistance was measured at 20 ± 0.5°C in a three-electrode cell containing a working ISE, a saturated silver–silver chloride reference electrode, and a platinum auxiliary electrode. The thickness of the membranes was measured micrometrically. The experimental data were processed according to [4].

To study ion transport through selective membranes, we used a cell whose design is presented in [5]. Transport properties of membranes, permeability coefficient P and ion flow J, were calculated by the following equations [5]:

$$\ln\left\{1 - \frac{2c_2^\tau}{c_1^0}\right\} = -2\pi d\frac{P}{V}\left(\frac{d}{2} + r\right)\tau, \quad (1)$$

$$J = P(c_1 - c_2), \quad (2)$$

where c_1 and c_2 are the concentrations of solutions that supply and receive ions in the corresponding compartments of the cell, respectively ($c_1 > c_2$, M); V is the volume of compartments (on condition that the volumes of the compartments containing the solutions that supply and receive ions are equal), m^3; d is membrane diameter, m; r is membrane thickness, m; c_1^0 is substance concentration in the solution that supplies ions at the time $\tau = 0$, M and; c_2^τ is substance concentration in the solution that supplies ions at a time $\tau > 0$, M.

To estimate the lipophilicity of tetraphenylborate derivatives and organic compounds, we calculated the values of log$P$, which represented the partition coefficient in the water–octanol system. Calculations were performed using the Chem 3D Ultra 8.0 program module of the Chem Office package of programs for molecular modeling and analysis (Cambridge Soft Corporation).

RESULTS AND DISCUSSION

Solubility of ionophores in water and conductivity of membranes. Table 1 shows that the solubility products of the ionophores under study decreased in the order $[B\{C_6H_3(CF_3)_2\}_4]^- \geq [B(C_6H_4Cl)_4]^- \geq [B(C_6H_4CH_3)_4]^- \geq [B(C_6H_5)_4]^-$ as the molecular mass and lipophilicity of tetraphenylborate derivatives increased. The calculated values of log$P$ for the above series were 14.63, 10.42, 9.56, and 7.57.

The studies of the specific conductivity of membranes (κ) as a function of their residence times in the solution showed that κ grew at the initial stage and then the conductivity of membranes was virtually unchanged with time. The growth of membrane conductivity with extension of the residence time of membranes in the solution is indicative of an increase in the fraction of charge carriers whose concentration was enhanced at the expense of both an increase in the permittivity of the membrane phase and extractive distribution involving the potential-determining ion present in the solution. Figure 2a presents the steady-state conductivity of the membrane based on $[C_{24}H_{32}O_4N]^+[B(C_6H_5)_4]^-$ as a function of the concentration of the near-membrane solution of $[C_{24}H_{32}O_4N]^+Cl^-$.

It is known [9–11] that, upon the exposure of a membrane to a solution, a 60-μm surface layer enriched with water is formed. The rate of its formation and the homogeneity of its distribution over the surface depend on the nature and concentration of the ion-exchanger. According to [10], the absorption of water by PVC membranes occurs at the expense of water salting. The highest concentration of the absorbed water is proportional to the diffusion coefficient and the concentration of the ion exchanger in the membrane:

$$\bar{c}_{H_2O} = \frac{D_{H_2O}^{obs}\bar{c}_{IS}}{D_{H_2O}^{obs} - D_{H_2O}}, \quad (3)$$

where $\bar{c}_{IS}$ is the concentration of the ion exchanger in the membrane and $D_{H_2O}^{obs}$ and D_{H_2O} are the observed and actual diffusion coefficients of water. The concentration of water in selective membranes based on PVC was on average ~1 wt % [12, 13].

According to Eq. (3), the equilibrium concentration of water in the membrane should be increased as the concentration of an ion exchanger is increased. Figure 2b, which indirectly demonstrates this, presents the relative permittivity ε_M^{rel} of membranes based on the ion

pair formed by $[C_{24}H_{32}O_4N]^+$ and $[B(C_6H_5)_4]^-$ as a function of the time of their contact with distilled water at different concentrations of the ion exchanger in the membrane.[1] For membranes with a higher concentration of the ion exchanger (Fig. 2b, curve *1*), ε_M^{rel} increased more sharply, which is indicative of an increase in the concentration of water absorbed by the membrane.

Electroanalytical properties of ISEs. First, we studied the effect of membrane composition on the electroanalytical properties of the ISE. It was found that background membranes did not respond to the drotaverine cation. When an ion exchanger was introduced into the ISE membrane as ion pairs containing $[C_{24}H_{32}O_4N]^+[B\{C_6H_{5-x}(R)_x\}_4]^-$ or $K^+[B\{C_6H_{5-x}(R)_x\}_4]^-$ structural units, the Nerstian dependence of potential on the $[C_{24}H_{32}O_4N]^+Cl^-$ concentration in the solution was observed. The character of the E–$(-\log c_{[C_{24}H_{32}O_4N]^+Cl^-})$ dependence, its linearity range, and the slope of this straight line depended on the concentration of the ion exchanger in the membrane phase. This is indicative of the reversible transfer of the $[C_{24}H_{32}O_4N]^+$ cation through the membrane–solution interface. The ISE electrode properties were optimum at a polymer (PVC)-to-plasticizer (DBP) ratio of 1 : (1.5–2.0) and at an ionophore concentration in the membrane of $(10–3.5) \times 10^{-3}$ mol/kg DBP. When the concentration of the ionophore decreased, the linearity range of the electrode response shifted to lower concentrations; however, the drift of potential with time became more significant, especially after several days of the extensive use of the ISE. At an ionophore concentration of lower than 1×10^{-3} mol/kg DBP, the slope of the electrode response and the stability of the ISE potential markedly decreased.

It follows from Table 2 that the linearity range of the electrode response widened and the detection limit lowered in the series of tetraphenylborate derivatives from $[B(C_6H_5)_4]^-$ to $[B\{C_6H_3(CF_3)_2\}_4]^-$, that is, with an increase in the molecular mass of the anion and a decrease in the ionophore solubility.

The linear dependence of the linearity range of the electrode response (ΔpC) on the solubility of the ion exchanger ($\sqrt{K_S^{IS}}$) was found earlier for membranes with the dispersed form of the ionophore [14].[2] A similar dependence (Fig. 3) was observed for the plasticized membranes based on ion pairs formed by drotaverine and tetraphenylborate derivatives. It is seen in Fig. 3 that the linearity range widened as the solubility of ionophores decreased.

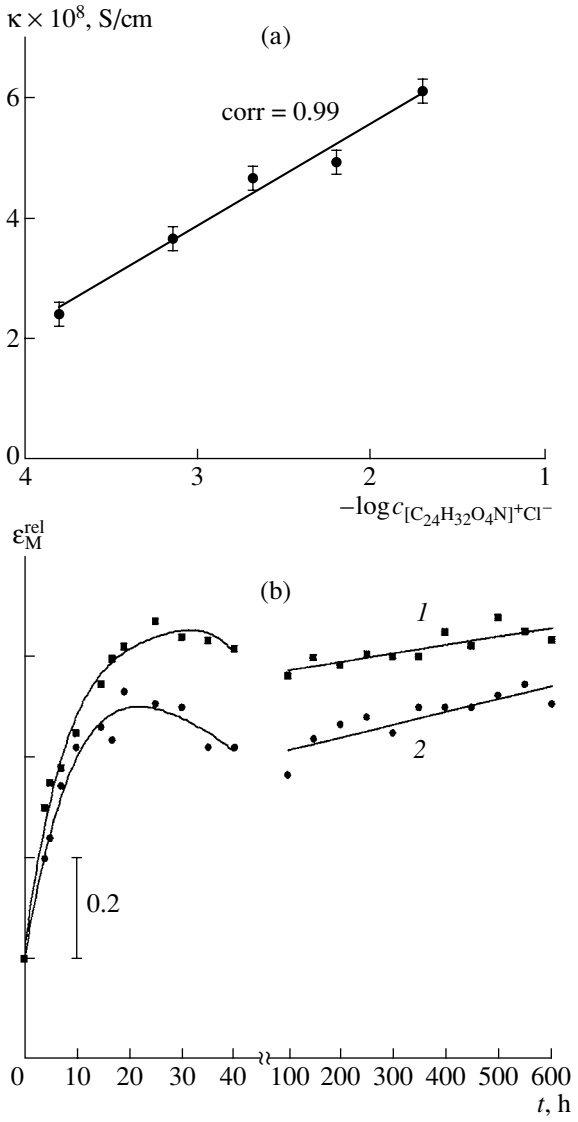

Fig. 2. (a) Steady-state conductivity as a function of the concentration of a $[C_{24}H_{32}O_4N]^+$ solution. (b) Relative permittivity of ion-selective membranes as a function of the time of membrane exposure to water (*1*, $\bar{c}_{[C_{24}H_{32}O_4N]^+[B(C_6H_5)_4]^-} = 1 \times 10^{-2}$ mol/kg DBP, $c_{[C_{24}H_{32}O_4N]^+Cl^-} = 0$; *2*, $\bar{c}_{[C_{24}H_{32}O_4N]^+[B(C_6H_5)_4]^-} = 1 \times 10^{-3}$ mol/kg DBP, $c_{[C_{24}H_{32}O_4N]^+Cl^-} = 0$).

The isothermic coefficients of ISEs $\left(\frac{dE}{dt}\right)$ were calculated from the calibration graphs in the temperature range from 25 to 60°C in accordance with [15]. For the electrodes based on the ion pairs formed by $[C_{24}H_{32}O_4N]^+$ and anions $[B(C_6H_5)_4]^-$, $[B(C_6H_4CH_3)_4]^-$,

[1] $\varepsilon_M^{rel} = |\varepsilon_M|^{t>0}/|\varepsilon_M|^{t=0}$, where $|\varepsilon_M|^{t=0}$ and $|\varepsilon_M|^{t>0}$ are the permittivities of the membrane before and after its contact with water, respectively.

[2] $\Delta pC = |\log(LBDC)| - |\log(UBDC)|$, where LBDC and UBDC are the lower and upper boundaries of determinable concentrations, respectively.

Table 2. Potentiometric characteristics of ISEs for determining drotaverine hydrochloride

ISE based on	Slope of the electrode response S, mV/pc	Linearity range, M	Detection limit, M
$[C_{24}H_{32}O_4N]^+[B(C_6H_5)_4]^-$	58 ± 2	5.0×10^{-2}–7.9×10^{-6}	$(4.3 \pm 0.2) \times 10^{-6}$
$[C_{24}H_{32}O_4N]^+[B(C_6H_4CH_3)_4]^-$	58 ± 1	5.0×10^{-2}–5.1×10^{-6}	$(1.3 \pm 0.3) \times 10^{-6}$
$[C_{24}H_{32}O_4N]^+[B(C_6H_4Cl)_4]^-$	60 ± 2	5.0×10^{-2}–8.2×10^{-7}	$(4.8 \pm 0.2) \times 10^{-7}$
$[C_{24}H_{32}O_4N]^+[B\{C_6H_2(CF_3)_3\}_4]^-$	61 ± 2	5.0×10^{-2}–4.8×10^{-7}	$(1.1 \pm 0.2) \times 10^{-7}$

$[B(C_6H_4Cl)_4]^-$, and $[B\{C_6H_3(CF_3)_2\}_4]^-$, they were 0.20 ± 0.02, 0.18 ± 0.03, 0.19 ± 0.02, and 0.19 ± 0.02 mV/°C, respectively. This is indicative of a rather high thermal stability of ISEs. When the system regained its original temperature, the electrode potentials coincided with the initial potentials, which confirmed the reversibility of the processes occurring in ISEs.

The time in which an equilibrium potential was attained is a very important characteristic of ISEs, particularly when they are used in flow-injection analysis (in this case, solid-state electrodes are meant) [16, 17]. The change in the ISE potential with time was studied at a concentration of the potential-determining ion in a test solution that was increased jumpwise in the ranges $(1 \longrightarrow 10) \times 10^{-5}$, $(1 \longrightarrow 10) \times 10^{-4}$, and $(1 \longrightarrow 10) \times 10^{-3}$ M. The time it took for the ISE potential to change by no more than ±1 mV was taken as the time in which the equilibrium potential was attained. Figure 4 presents the time dependence of ISE potential at a concentration of $[C_{24}H_{32}O_4N]^+Cl^-$ that was changed jumpwise.

It follows from the effect of the pH of a $[C_{24}H_{32}O_4N]^+Cl^-$ solution on the ISE potential (Fig. 5) that all ISEs under study operated almost in the same pH range (1.8–6.5). At pH > 7, potential decreased because the concentration of potential-determining ions lowered as a result of the deprotonation of the $[C_{24}H_{32}O_4N]^+$ cation and the formation of $C_{24}H_{31}O_4N$ precipitate that was responsible for the turbidity of the solution. In a strongly acidic solution at pH < 1, the change in the ISE potential was, evidently, due to incidental processes involving H^+ ions.

The potentiometric selectivity coefficients of the drotaverine-SE with respect to different interfering ions are presented in Fig. 6. It follows from Fig. 6 that Na^+, K^+, Mg^{2+}, Ca^{2+}, and some organic compounds did not affect the ISE potential. Of organic cations, the highly hydrophobic cetylpyridinium cation that possesses surfactant properties had a significant effect on the ISE

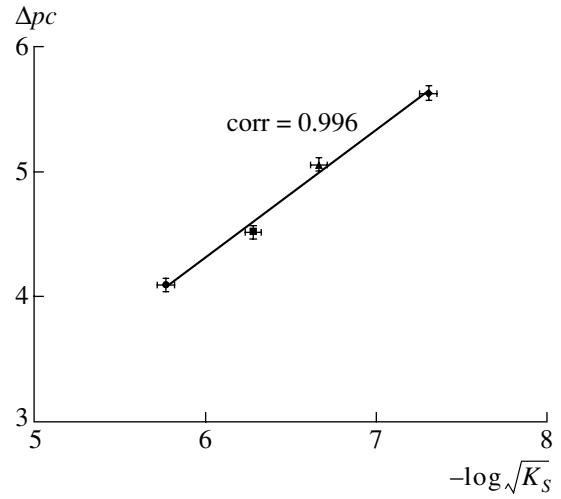

Fig. 3. The linearity range of the electrode response (ΔpC) as a function of the solubility of ionophoric components of ISE membranes based on (dark circles) $[C_{24}H_{32}O_4N]^+[B(C_6H_5)_4]^-$, (dark squares) $[C_{24}H_{32}O_4N]^+[B(C_6H_4CH_3)_4]^-$, (dark triangles) $[C_{24}H_{32}O_4N]^+[B(C_6H_4Cl)_4]^-$, and (dark rhombs) $[C_{24}H_{32}O_4N]^+[B\{C_6H_3(CF_3)_2\}_4]^-$.

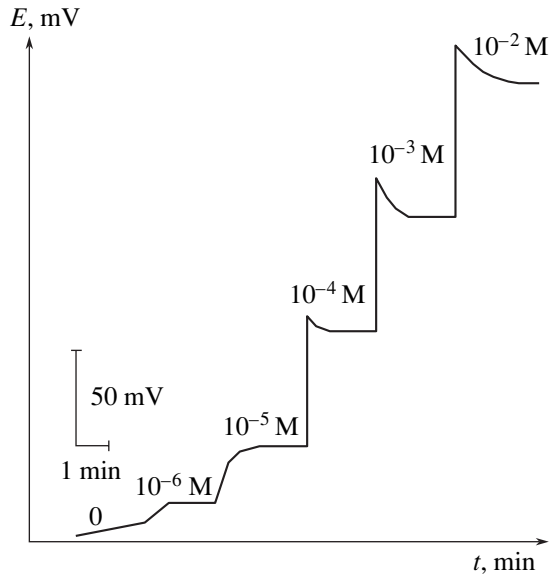

Fig. 4. Time dependence of the potential of the ISE based on $[C_{24}H_{32}O_4N]^+[B(C_6H_5)_4]^-$ at a jumpwise increased concentration of the potential-determining ion in the solution.

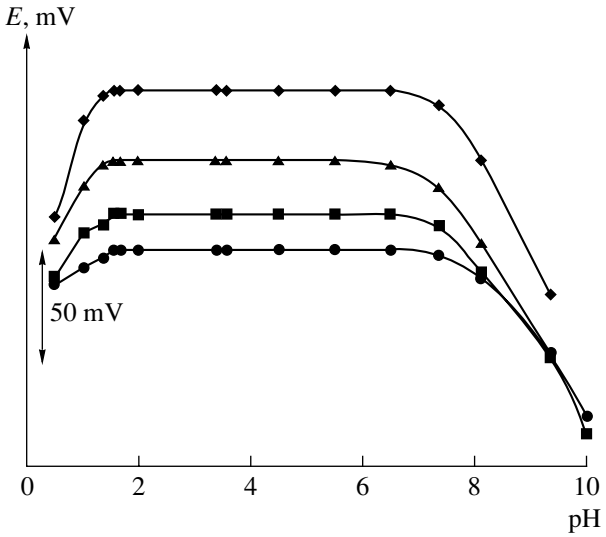

Fig. 5. Effect of pH on the potential of ISE based on (dark circles) $[C_{24}H_{32}O_4N]^+[B\{C_6H_2(CF_3)_3\}_4]^-$, (dark squares) $[C_{24}H_{32}O_4N]^+[B(C_6H_4Cl)_4]^-$, (dark triangles) $[C_{24}H_{32}O_4N]^+[B(C_6H_4CH_3)_4]^-$, and (dark rhombs) $[C_{24}H_{32}O_4N]^+[B(C_6H_5)_4]^-$.

selectivity. In this case, the membrane potential resulted from the electrostatic interaction between the surfactant and ion-exchanger active sites of the membrane; the ISE characteristics were mainly governed by the hydrophobicity of the interfering ion. The hydrophobicity of the interfering ion had a detrimental effect on the potentiometric response of the ISE because of the considerable adsorption of this ion on the membrane surface.

Transport and adsorption properties of selective membranes. The main transport properties of selective membranes, permeability coefficient P and the flow of ions J, were calculated by equations (1) and (2) for membranes based on $K^+[B\{C_6H_{5-x}(R)_x\}_4]^-$ ion exchangers.

Table 3 presents the values of P and J for membranes based on different tetraphenylborate derivatives with respect to drotaverine hydrochloride at a given concentration of the ion exchanger in the membrane and at a constant concentration of the solution in the cell compartment that supplied potential-determining ions. The values of P and J increased in going from less lipophilic tetraphenylborate derivatives to more lipophilic derivatives in the series $[B(C_6H_5)_4]^- <$

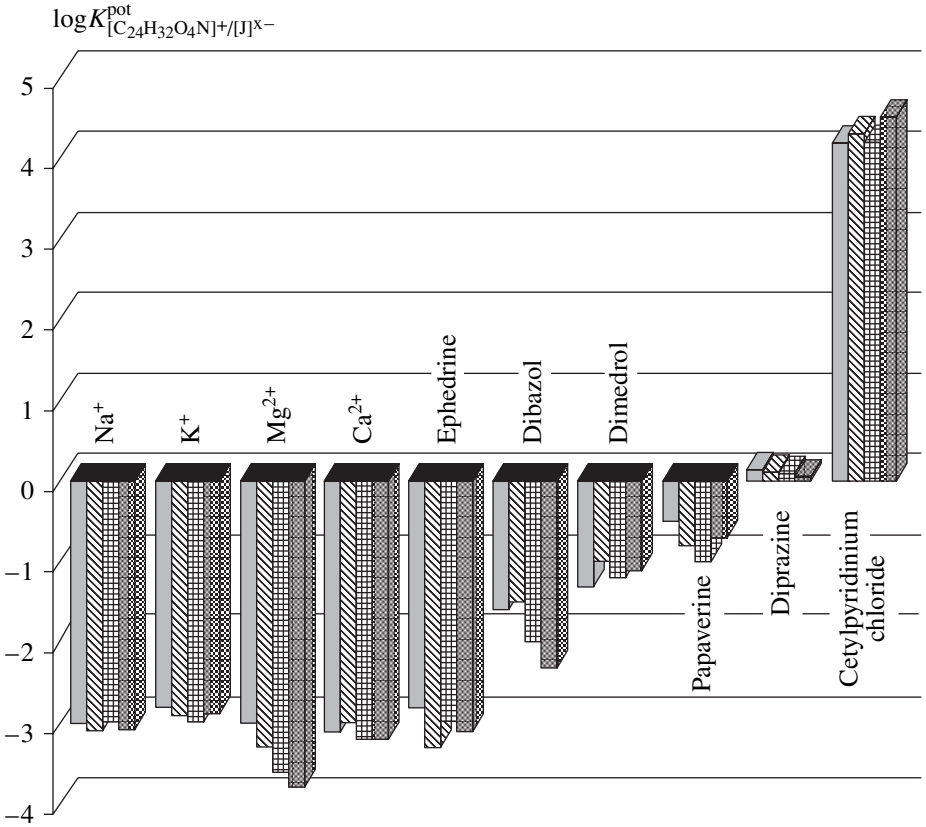

Fig. 6. Dependence of the logarithms of potentiometric selectivity coefficients on the nature of interfering ions for ISEs based on (▢) $[C_{24}H_{32}O_4N]^+[B(C_6H_5)_4]^-$, (▧) $[C_{24}H_{32}O_4N]^+[B(C_6H_4CH_3)_4]^-$, (▦) $[C_{24}H_{32}O_4N]^+[B(C_6H_4Cl)_4]^-$, and (▩) $[C_{24}H_{32}O_4N]^+[B\{C_6H_2(CF_3)_3\}_4]^-$.

Table 3. Permeability coefficient (P) and ion flow (J) as functions of the nature of ion exchanger in the membrane at $\bar{c}$ $[C_{24}H_{32}O_4N]^+Cl^- = 1.0 \times 10^{-3}$ M and $\bar{c}$ $K^+[B\{C_6H_{5-x}(R)_x\}_4]^- = 1.0 \times 10^{-2}$ mol/kg DBP

Active group of ion exchanger	Permeability coefficient P, m/s	Flow of ions J, mol/m^2 s
$[B(C_6H_5)_4]^-$	3.7×10^{-8}	8.6×10^{-8}
$[B(C_6H_4CH_3)_4]^-$	9.7×10^{-8}	2.3×10^{-7}
$[B(C_6H_4Cl)_4]^-$	3.1×10^{-7}	7.8×10^{-7}
$[B\{C_6H_2(CF_3)_3\}_4]^-$	6.4×10^{-7}	1.5×10^{-6}

$[B(C_6H_4CH_3)_4]^- < [B(C_6H_4Cl)_4]^- < [B\{C_6H_3(CF_3)_2\}_4]^-$. This indicates that the active group of the ion exchanger participated directly in the transfer of counterions through the membrane.

In our case, the ion exchanger introduced into the membrane before its contact to the solution was in the form of potassium salt $K^+[B\{C_6H_{5-x}(R)_x\}_4]^-$. Two main factors, the process of extractive distribution

$$[C_{24}H_{32}O_4N]^+ \rightleftharpoons \overline{[C_{24}H_{32}O_4N]^+} \quad (4)$$

and the process of easier diffusion, will contribute to the transfer of $[C_{24}H_{32}O_4N]^+$ ions through the membrane.[3] The active group of the $[B\{C_6H_{5-x}(R)_x\}_4]^-$ ion exchanger that is responsible for the selective conductivity of the membrane forms the ion pair with $[C_{24}H_{32}O_4N]^+$ ion at its surface by the exchange reaction

$$\begin{aligned}&[C_{24}H_{32}O_4N]^+ + \overline{K^+[B\{C_6H_{5-x}(R)_x\}_4]^-} \\ &\rightleftharpoons K^+ + \overline{[C_{24}H_{32}O_4N]^+[B\{C_6H_{5-x}(R)_x\}_4]^-}.\end{aligned} \quad (5)$$

The complex formed is sufficiently mobile and, moving to the opposite surface of the membrane, releases $[C_{24}H_{32}O_4N]^+$ ions to the aqueous phase. $[B\{C_6H_{5-x}(R)_x\}_4]^-$ ions return back under the action of a magnetic field.

Figure 7a presents permeability coefficient as a function of the ion-exchanger concentration. It follows from Fig. 7a that, at low concentrations of $K^+[B\{C_6H_{5-x}(R)_x\}_4]^-$, coefficient P increased insignificantly; then, it grew linearly, and, at high concentrations of the carrier, reached some limiting value.

It was found earlier that the transport of counterions in selective membranes based on ion pairs was due to diffusion and migration transfer, release, and extractive distribution [5]. In the absence of an ion exchanger or at its low concentrations (Fig. 7a, region A), the transfer was accomplished by the extractive distribution of the electrolyte in the phase of the membrane solvent. As the concentration of the carrier in the membrane increased, the fraction of active ion-exchanger sites also increased, which favored the transfer of the counterion by the appearing concentration gradient (Fig. 7a, region B). At a rather high concentration of the ion exchanger in the membrane, the diffusion of ions inside the membrane became the limiting stage of the transfer, as will be shown below. As a result, the transfer rate decreased and the curve of the P–c $\bar{c}_{K^+[B\{C_6H_{5-x}(R)_x\}_4]^-}$ dependence flattened out (Fig. 7a, region C).

The ion flow as a function of the concentration of the near-membrane $[C_{24}H_{32}O_4N]^+Cl$ solution is shown in Fig. 7b. It follows from Fig. 7b that, at a concentration of the near-membrane solution higher than 3×10^{-2} M, the flow of ions J almost ceased to increase and reached the limiting value. According to [18], for the solutions with low concentrations, in the majority of cases, the diffusion through the aqueous boundary layer formed at the membrane surface during its exposure to the solution is the limiting stage of the adsorption transfer. In the solutions with rather high concentrations, diffusion inside the membrane becomes the limiting stage. The rate of transfer by diffusion inside the membrane is lower than the rate of transfer by diffusion through the aqueous boundary layer [18], because the membrane phase is more viscous than the solution and is not stirred. This retards the transport of ions through the membrane, so that the ion flow approaches a somewhat constant value. For highly hydrophobic organic ions, the rate of extraction–adsorption transfer may be restricted not only by the diffusion mechanism, but also directly by the rate of an ion-exchange act [19].

The kinetics of interrupted ion-exchange adsorption was studied to establish the presence of limiting stages of diffusion through the aqueous boundary layer and inside the membrane. For this purpose, we first found the time it took to attain equilibrium (5). The membrane containing the $K^+[B\{C_6H_{5-x}(R)_x\}_4]^-$ ion exchanger was placed in a solution of $[C_{24}H_{32}O_4N]^+Cl$ with a known concentration, and samples of this solution were taken at certain intervals while periodically stirring the solution to determine the concentration of $[C_{24}H_{32}O_4N]^+Cl$. Next, a similar experiment was carried out with a new membrane with the difference that, before the equilibrium was attained in the system, the contact between the membrane and the solution was interrupted (the membrane was removed from the solution), and, after a lapse of time (5), the phases were again connected and the time dependence of the $[C_{24}H_{32}O_4N]^+Cl^-$ concentration was studied further. The experiment was repeated for different concentrations of

[3] The upper line designates that the substance belongs to the membrane phase.

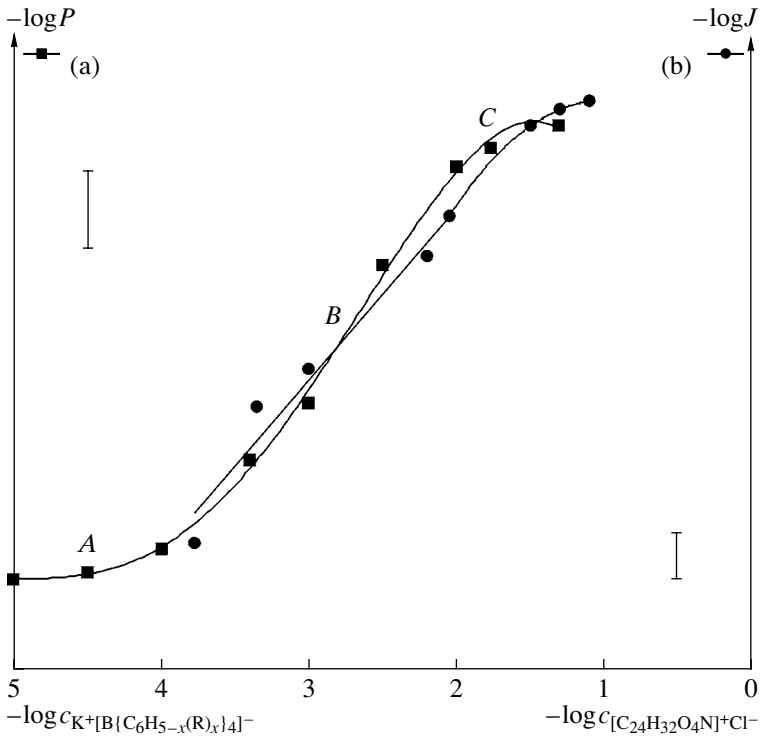

Fig. 7. (a) Permeability coefficient as a function of the concentration of ion exchanger in the membrane and (b) ion flow as a function of the concentration of $[C_{24}H_{32}O_4N]^+Cl^-$ in the near-membrane solution.

the near-membrane solution and at different concentrations of the ion exchanger in the membrane. Conversion F as a function of the experimental time t for different concentrations $c_{[C_{24}H_{32}O_4N]^+Cl^-}$ and $\bar{c}_{K^+[B\{C_6H_{5-x}(R)_x\}_4]^-}$ is presented in Fig. 8.[4]

According to Fig. 8, at a $[C_{24}H_{32}O_4N]^+Cl^-$ concentration of 1×10^{-3} M, after interrupting the contact between the membrane and the solution, the curve was virtually unchanged. In this case, the gradient of the $[C_{24}H_{32}O_4N]^+$ concentration in the membrane was absent from the very beginning, and the diffusion of ions through the aqueous boundary layer (film) was the limiting stage. For higher concentrations of both the near-membrane solution (5.5×10^{-2} M; Fig. 8, curve *2*) and the ion exchanger in the membrane phase (curve *3*), gradients of concentrations that arose in the membrane during interrupting the contact between phases had time to lower so that the rate of the ion exchange (5) after restoring the contact corresponded to a smaller fraction of conversion as compared to that at the instant the contact was interrupted, and diffusion of ions inside the membrane became the limiting stage in this case.

Thus, as shown above, for different concentrations of the near-membrane solution and the ion exchanger in the membrane phase, the rate of the extraction–adsorption transfer of $[C_{24}H_{32}O_4N]^+$ was limited either by the diffusion of ions through the boundary layer or by diffusion in the membrane, which affected the values of permeability coefficients and the ion flow.

It follows from the dependence of permeability coefficient P on the membrane thickness r (Fig. 9) that, with an increase in r, the permeability coefficient decreased according to Eq. (1). The P–r dependence can be satisfactorily described by a linear equation, which is indicative of the decisive contribution of the passive transport of ions to the process of their transfer.

Analytical application of the ISE. ISEs reversible to the $[C_{24}H_{32}O_4N]^+$ cation possess quite acceptable electroanalytical properties and performance characteristics and may be recommended for determining drotaverine hydrochloride in different pharmaceutical forms by potentiometry and potentiometric precipitation titration.

For the potentiometric determination of drotaverine hydrochloride, a tablet of a preparation (or a solution from an ampoule) was transferred to a 50.0-mL volumetric flask placed in a shaker. The shaker was switched on and operated until the tablet was completely disintegrated. The obtained turbid solution whose turbidity was due to the presence of a filler that

[4] Conversion F is the ratio between the concentration of the exchanging ion at instant t to the concentration of the exchanging ion in the equilibrium state. $F = \left|\bar{c}_{[C_{24}H_{32}O_4N]^+}\right|^{t \geq 0} \Big/ \left|\bar{c}_{[C_{24}H_{32}O_4N]^+}\right|^{t = \infty}$.

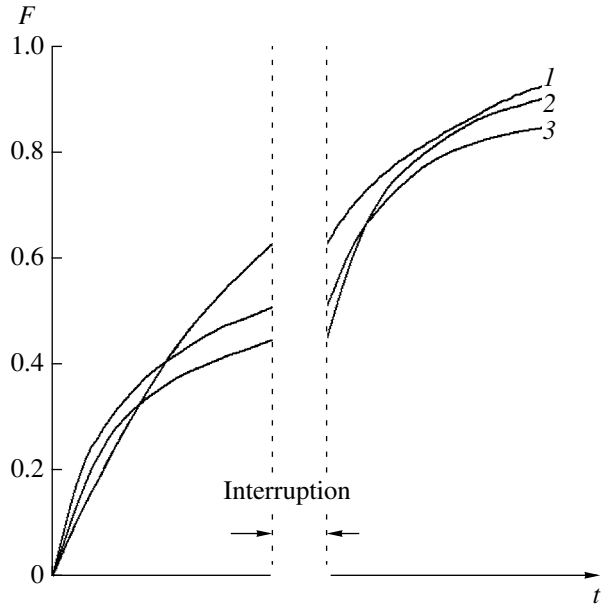

Fig. 8. Curves of $[C_{24}H_{32}O_4N]^+Cl^-$ adsorption on the membranes with the $K^+[B\{C_6H_{5-x}(R)_x\}_4]^-$ form of ion exchanger. The experiment on interruption. (*1*, $c_{[C_{24}H_{32}O_4N]^+Cl^-} = 1.0 \times 10^{-3}$ M, $\bar{c}_{K^+[B\{C_6H_{5-x}(R)_x\}_4]^-} = 5.0 \times 10^{-4}$ mol/kg DBP; *2*, $c_{[C_{24}H_{32}O_4N]^+Cl^-} = 5.5 \times 10^{-2}$ M, $\bar{c}_{K^+[B\{C_6H_{5-x}(R)_x\}_4]^-} = 5.0 \times 10^{-4}$ mol/kg DBP; and *3*, $c_{[C_{24}H_{32}O_4N]^+Cl^-} = 5.0 \times 10^{-2}$ M, $\bar{c}_{K^+[B\{C_6H_{5-x}(R)_x\}_4]^-} = 1.0 \times 10^{-2}$ mol/kg DBP).

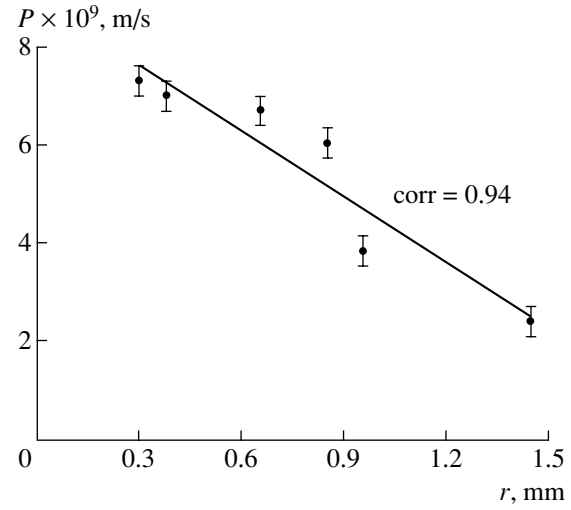

Fig. 9. Permeability coefficient *P* as a function of the membrane thickness *r*.

did not interfere with the determination of the analyte was diluted to the mark with distilled water and stirred. A portion of the solution was transferred to the cell, and the emf of the cell containing the reference electrode and the corresponding ISE was measured. The concentration of drotaverine hydrochloride was found from the calibration graph.

For the potentiometric precipitation titration of drotaverine hydrochloride, a tablet of the preparation (or a solution from an ampule) was transferred to a beaker, 10 mL of warm distilled water was added, and the beaker was allowed to stand until the tablet was completely disintegrated. The indicator ISE and the reference electrode filled with a saturated sodium chloride solution were immersed into the cell. A magnetic stirrer was switched on, and the solution was titrated with a 0.05 M sodium tetraphenylborate solution using a micropipette. The amount of drotaverine hydrochloride (g) in a pharmaceutical form was calculated by the equation

$$m = 0.4340 c_M^{NaTPB} V_E^{NaTPB},$$

where c_M^{NaTPB} is the accurate concentration of the titrant M, and V_E^{NaTPB} is the volume of the NaTPB solution consumed in the titration of the aliquot of the solution, mL.

Table 4 presents the results of determining drotaverine hydrochloride in pharmaceutical forms by potentiometry and HPLC. The accuracy and sensitivity of the proposed procedures for the potentiometric determination of the drug are quite acceptable, and these procedures are much simpler in instrumentation and, therefore, are more available.

Table 4. Comparison of the results of determining drotaverine hydrochloride in pharmaceutical forms by HPLC and potentiometry with the ISE based on the $[C_{24}H_{32}O_4N]^+[B(C_6H_5)_4]^-$ ion pair

Pharmaceutical form	Found, $(g \pm \delta) \times 10^2$		Potentiometric precipitation titration	
	direct potentiometry	HPLC	DH concentration, $g \times 10^2$	found, $\% \pm \delta$
Solution for injections (2%)	4.10 ± 0.06	3.98 ± 0.03	4.0	100.4 ± 0.6
NO-SPA tablets	4.08 ± 0.05	4.01 ± 0.02	4.0	99.7 ± 0.5
Nikoshpan tablets	7.76 ± 0.07	7.79 ± 0.02	7.8	99.6 ± 0.6
Bishpan tablets	5.78 ± 0.05	6.04 ± 0.02	6.0	100.5 ± 0.6

Note: RSD = 1.1% in the method of direct potentiometry and RSD = 0.34% in the method of potentiometric titration.

REFERENCES

1. Mashkovskii, M.D., *Lekarstvennye sredstva* (Drugs), Moscow: Meditsina, 1985.
2. Bolaji, O.O., Onyeji, C.O., Ogungbamila, F.O., and Ogunbona, F.A., *J. Chromatogr., Biomed. Appl.,* 1993, vol. 622, no. 1, p. 93.
3. Lalla, J.K., Shah, M.U., Jain, M.B., and Sharma, A.H., *J. Pharm. Biomed. Anal.*, 1993, vol. 11, nos. 4–5, p. 385.
4. Buck, R.P. and Mundt, C., *Electrochim. Acta,* 1999, vol. 44, no. 12, p. 1999.
5. Kharitonov, S.V., *Zh. Anal. Khim.*, 2003, vol. 58, no. 2, p. 199 [*J. Anal. Chem.* (Engl. Transl.), vol. 58, no. 2, p. 176].
6. Mishchenko, K.P. and Poltoratskii, T.M., *Voprosy termodinamiki i stroeniya vodnykh rastvorov* (Thermodynamic Aspects of the Structure of Aqueous Solutions), Leningrad: Khimiya, 1968.
7. Eugster, R., Rosatzin, T., Rusterholz, B., Aebersold, B., Pedrazza, U., Ruegg, D., Schmid, A., Spichiger, U.E., and Simon, W., *Anal. Chim. Acta,* 1994, vol. 289, no. 1, p. 1.
8. Tinius, K., *Plastifikatory* (Plasticizers), Moscow: Khimiya, 1964.
9. Li, Z., Li, X., Petrovic, S., and Harrison, D.J., *Anal. Meth. Instrum.,* 1993, vol. 1, no. 1, p. 30.
10. Li, Z., Li, X., Petrovic, S., and Harrison, D.J., *Anal. Chem.,* 1996, vol. 68, no. 10, p. 1717.
11. Li, Z., Li, X., Rothmaier, M., and Harrison, D.J., *Anal. Chem.*, 1996, vol. 68, no. 10, p. 1726.
12. Boldurin, W.H., Higgins, C.E., and Soldano, B.A., *J. Phys. Chem.*, 1959, vol. 63, no. 1, p. 118.
13. Thoma, A.P., Vivani-Nauer, A., Arvanitis, S., Morf, W.E., and Simon, W., *Anal. Chem.*, 1977, vol. 49, no. 11, p. 1567.
14. Kharitonov, S.V., *Anal. Bioanal. Chem.*, 2005, vol. 382, no. 7, p. 1642.
15. Oesch, V., Ammann, D., and Simon, W., *Clin. Chem.*, 1986, vol. 32, no. 8, p. 1148.
16. Buck, R.P. and Lindner, E., *Pure Appl. Chem.*, 1994, vol. 66, no. 12, p. 2527.
17. Buck, R.P. and Cosofret, V.V., *Pure Appl. Chem.,* 1993, vol. 65, no. 8, p. 1849.
18. Helfferich, F., *Ionenaustauscher*, Weinheim: Chemie, 1959.
19. Millar, J.R., Smith, D.G., Marr, W.E., and Kressman, T.R.E., *J. Chem. Soc.*, 1963, vol. 515.